Progress on Modelling of $Pb_{83}Li_{17}$ Recondensation on INPORT Units

L. Pong, D.K. Sze, R.R. Peterson, G.A. Moses

August 1982

FPA-82-5

FUSION POWER ASSOCIATES

2 Professional Drive, Suite 248
Gaithersburg, Maryland 20879
(301) 258-0545

1500 Engineering Drive
Madison, Wisconsin 53706
(608) 263-2308

Progress on Modeling of $Pb_{83}Li_{17}$ Recondensation on INPORT Units

L.C. Pong

D.K. Sze

R.R. Peterson

G.A. Moses

July 1982

FPA-82-5

Abstract

In the HIBALL heavy ion beam fusion reactor design, the INPORT concept is used to protect the first surface of the reactor from being damaged by the high energy x-rays, ion debris and fast neutrons from the exploding target. Liquid $Pb_{83}Li_{17}$ flows through porous SiC tubes and wets the outside of the tubes with a layer of $Pb_{83}Li_{17}$. This $Pb_{83}Li_{17}$ film is evaporated on each shot by the target x-rays and ion debris. The mechanisms that control the vapor pressure of the chamber are: gas radiation, $Pb_{83}Li_{17}$ evaporation from the INPORT tubes, and gas condensation back onto the INPORT tubes. From the beam stripping cross section for Bi^{2+} ions on Pb we know that the gas density inside the chamber must be at or below $4 \times 10^{10}/cm^3$ in order for the ion beam to reach the target and ignite it. Also from the time that the vapor takes to recondense we can determine the allowable repetition rate of the reactor.

I. Introduction

HIBALL[1] (Heavy Ion Beam and Lithium Lead) is a conceptual reactor design for inertial confinement fusion (ICF) with beams of heavy ions. The reactor chamber is shown in Fig. 1. Some of the operating parameters of the reactor chamber are listed in Table 1. A persistent technical problem in the ICF field has been the protection of the first load bearing walls from high energy target debris, x-rays and neutrons. The INPORT concept[2] (Inhibited Flow-Porous Tube) was proposed in the HIBALL design to meet this requirement and to prolong the lifetime of the reactor cavities.

The INPORT tube is a woven SiC tube, acting as the first structure facing the fusion products (see Fig. 2). It is flexible, sufficiently strong, compatible with $Pb_{83}Li_{17}$, and loose enough to allow some of the liquid metal to leak out from the tube and wet the outside of the tube. The thickness of the film (~ 1 mm) is enough to absorb the x-rays and debris from the target explosion in order to reduce the heat load of the outside structure. After absorbing this energy, the liquid film is evaporated and produces a dense gas inside the reactor chamber. The amount of vaporized mass is determined by the target design and target x-ray spectrum. In order for 80% of the ion beam to transport and hit the target, the pressure inside the cavity should be lower than $4 \times 10^{10}/cm^3$.[1] That means we have to wait until the cavity pressure is low enough for the next shot. The objective of this study is to understand the gas pressure history of the cavity. After this is well understood, we will be able to explore the cavity response to different target designs and compare the maximum repetition rate associated with each target design. Then we can determine the most suitable target design for the reactor. This report

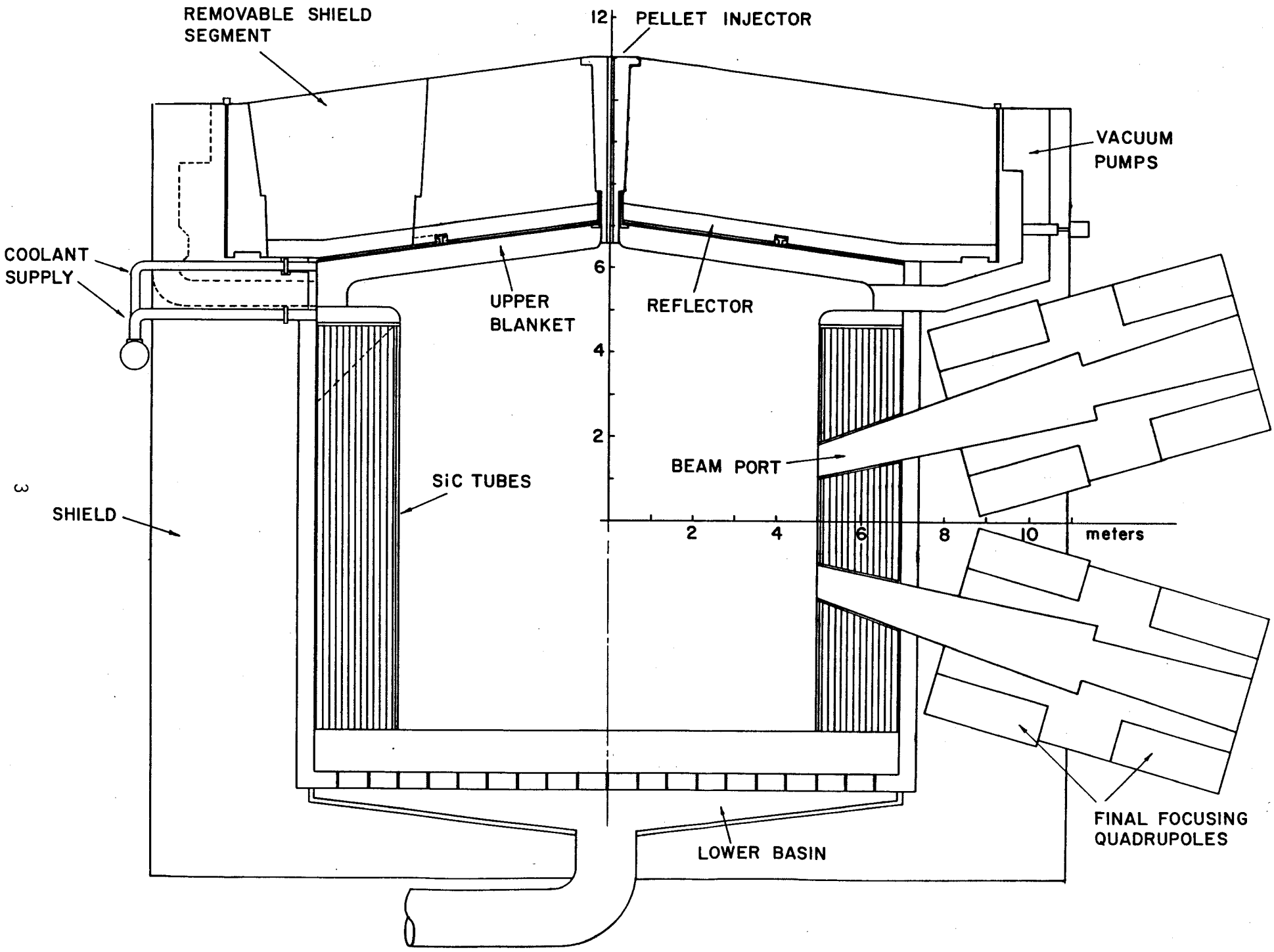

Figure 1 Cross Sectional View of HIBALL Reaction Chamber

Table 1. Selective Operating Parameters of HIBALL Reaction Chamber

Target Yield	400 J
X-ray and Ion Debris Energy to First Tube Bank	35 J/cm^2
INPORT Tube Length	10 m
INPORT Tube Outer Radius	
(inner rows)	1.5 cm
(outer rows)	5 cm
Amount of $Pb_{83}Li_{17}$ Evaporated Per Shot	13 kg

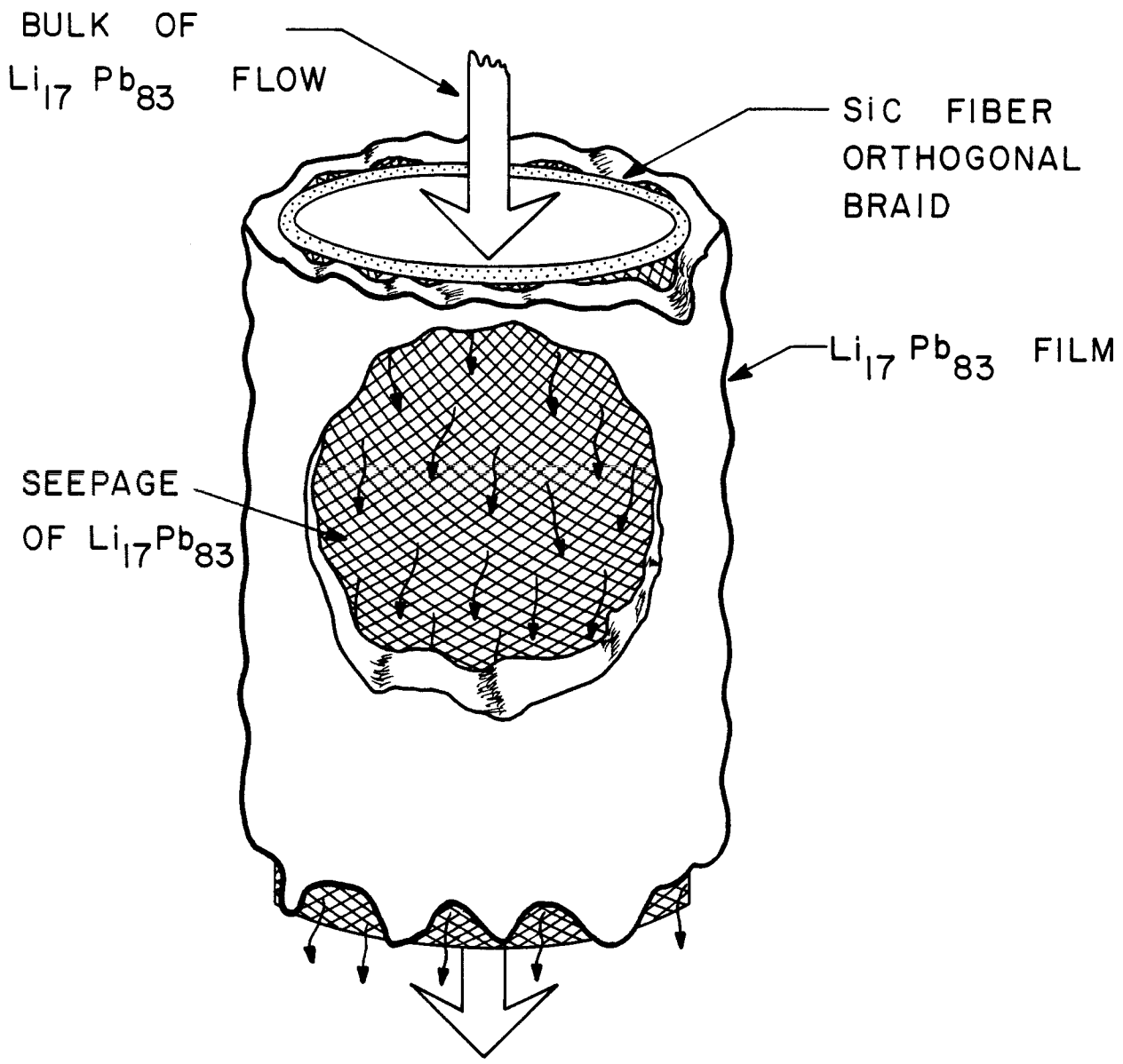

Figure 2 Schematic of INPORT concept. Metallic coolant seeps through porous woven structure to protect outside of tube from target x-ray and ion debris.

represents a summary of work completed between the HIBALL report[1] and the current date. A vigorous effort is continuing in this area.

The whole gas dynamics sequence is shown in Fig. 3 (this comes from our calculation results). After a target explosion, the x-ray energy is deposited in 10^{-3} cm of the liquid film, which is flowing down the outside of the SiC porous tubes. The temperature of the $Pb_{83}Li_{17}$ is raised above its boiling temperature and the $Pb_{83}Li_{17}$ is vaporized. The evaporated Li and Pb vapor flow into the chamber and their temperature is further raised by absorbing the energy of the debris. Thus the first surface is also protected from the energetic ion debris. The hot gas then starts to radiate energy back to the INPORT tubes, causing additional $Pb_{83}Li_{17}$ to be evaporated into the chamber. The radiational heat will decrease because of the bulk gas cooling, and also because of the increasing gas opacity from the addition of mass. The cooling gas will condense back on the surface and deposit its energy, resulting in further $Pb_{83}Li_{17}$ evaporation.

The gas density is quite high after the initial x-ray deposition, and varies by the coupled effects of condensation and evaporation. For the target and debris spectra of HIBALL, a total of 13 kg of $Pb_{83}Li_{17}$ was calculated to be evaporated.[3] We have calculated the gas radiation, condensation and evaporation mechanisms based on the following conditions and assumptions:

1. By neglecting the curvature effect of the reactor chamber, we did a one-dimensional calculation.
2. Since the mass fraction of Li in the $Pb_{83}Li_{17}$ alloy is quite small ($\sim$ 0.6%), we assume all radiation, condensation and evaporation are due to Pb only.
3. The thermophysical properties of $Pb_{83}Li_{17}$ are independent of temperature.

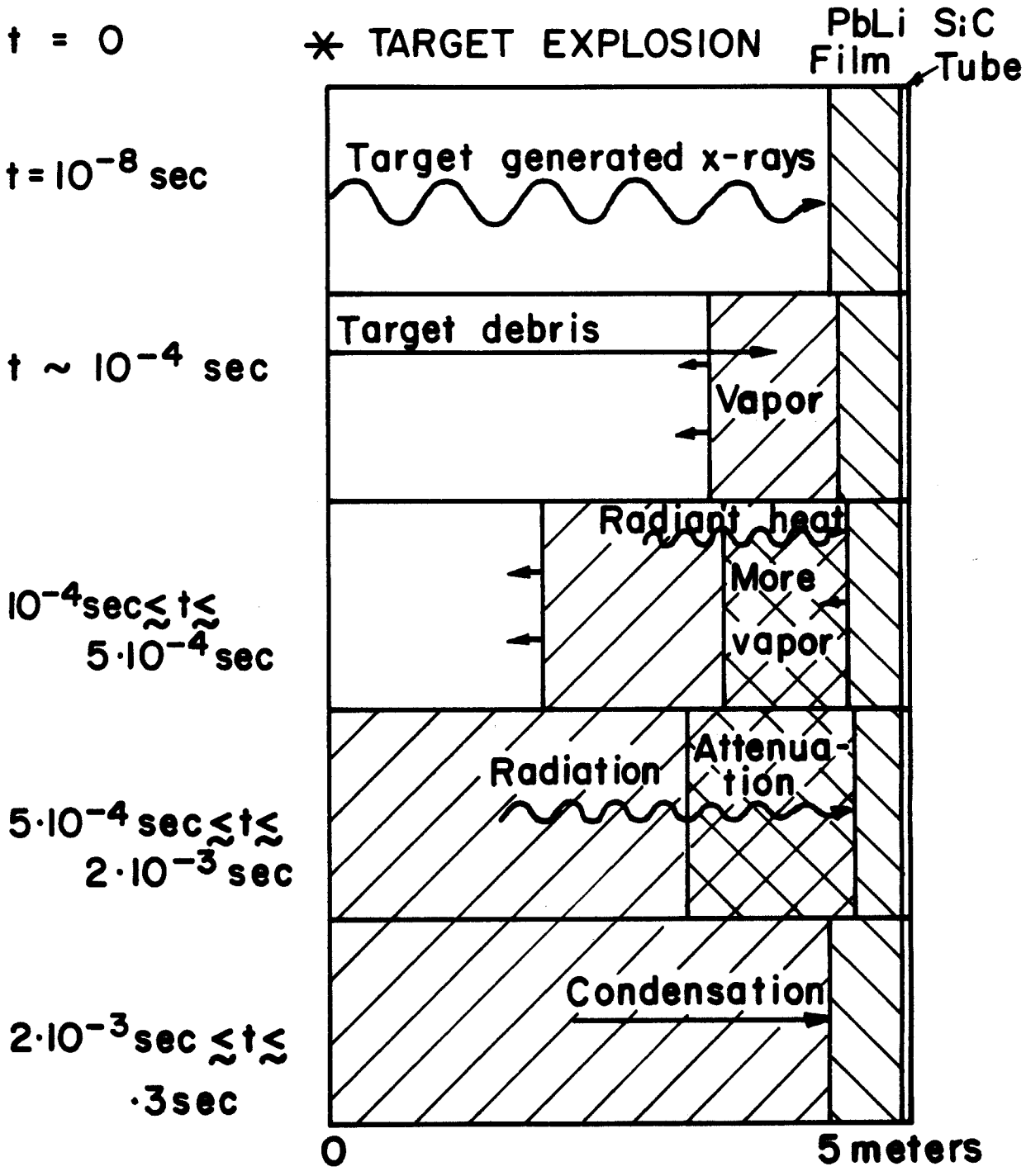

Figure 3 History of the $Li_{17}Pb_{83}$ Vapor

4. This calculation begins right after the liquid $Pb_{83}Li_{17}$ is blown off from the surface by absorption of the high energy x-rays.
5. The ionization of the gas is assumed to occur in either Saha[5] or Coronal[6] model.
6. The radiative processes follow a semi-classical formalism.[7]
7. Condensation and evaporation happen within a few mean free paths from the liquid film.
8. According to its kinetic energy, the evaporated mass is assumed to stop in a certain ρR and uniformly distributes into this region.
9. Assume the conditions (pressure, temperature) of the liquid film are in static thermal equilibrium.
10. Assume all the molecules approaching the surface will condense, and all the molecules leaving the surface will eventually escape from the surface, neglecting the collisions between the condensed and evaporated particles.
11. Neglect the noncondensible gas (D, T, He) effect on the heat and mass transfer.
12. The thickness of the film is 1.5 mm.
13. Coolant temperature is 324°C and the heat transfer coefficient is 12 W/cm^2 °C.

The analysis has been achieved with several coupled computer codes. We obtained the x-ray spectrum from a target burn simulation.[1] Deposition of the x-rays and creation of the vapor were modeled by an x-ray stopping code.[3] A radiation hydrodynamics code[4] was used to model the gas flow and radiation transfer. The condensation and evaporation were analyzed with a heat transfer code that was recently incorporated into the hydrodynamics code.

We list the governing equations and describe the improvements we made since the last publication[3] in Section II. Section III presents the results of the calculation for 13 kg initially evaporated mass. In Section IV, the conclusion and comments are addressed.

II. Improvements and the Listing of Governing Equations

The major changes compared to our previous calculations are:

(a) Combined gas radiation, evaporation and condensation effects. Before we first assumed the gas density was uniform, then calculated the history of radiation heat flux and the gas temperature from the FIRE[4] code. Using those data as the input to the first surface, we calculated the $Pb_{83}Li_{17}$ condensation and evaporation. This method is inconsistent since the evaporated and condensed mass will have a significant effect on the gas radiation, so in this calculation we combined those effects. The exchange of mass and energy between the bulk gas and the first surface is shown in Fig. 4. Q is the heat flux due to radiation, condensation or evaporation. G is the mass flux leaving or arriving at the surface. P, T are the pressure and temperature.

(b) Use a better model to modify the ionization state. We use both the Coronal and Saha models to describe the ionization at low and high gas density. This provides us with a more accurate set of data compared to before for charge state, specific internal energy, Rosseland mean free path and Planck mean free path. For example, the charge state is shown in Fig. 5. The black line separates the regions in which either the Coronal or Saha model dominates.

The governing equations for heat and mass transfer, and condensation and evaporation are:

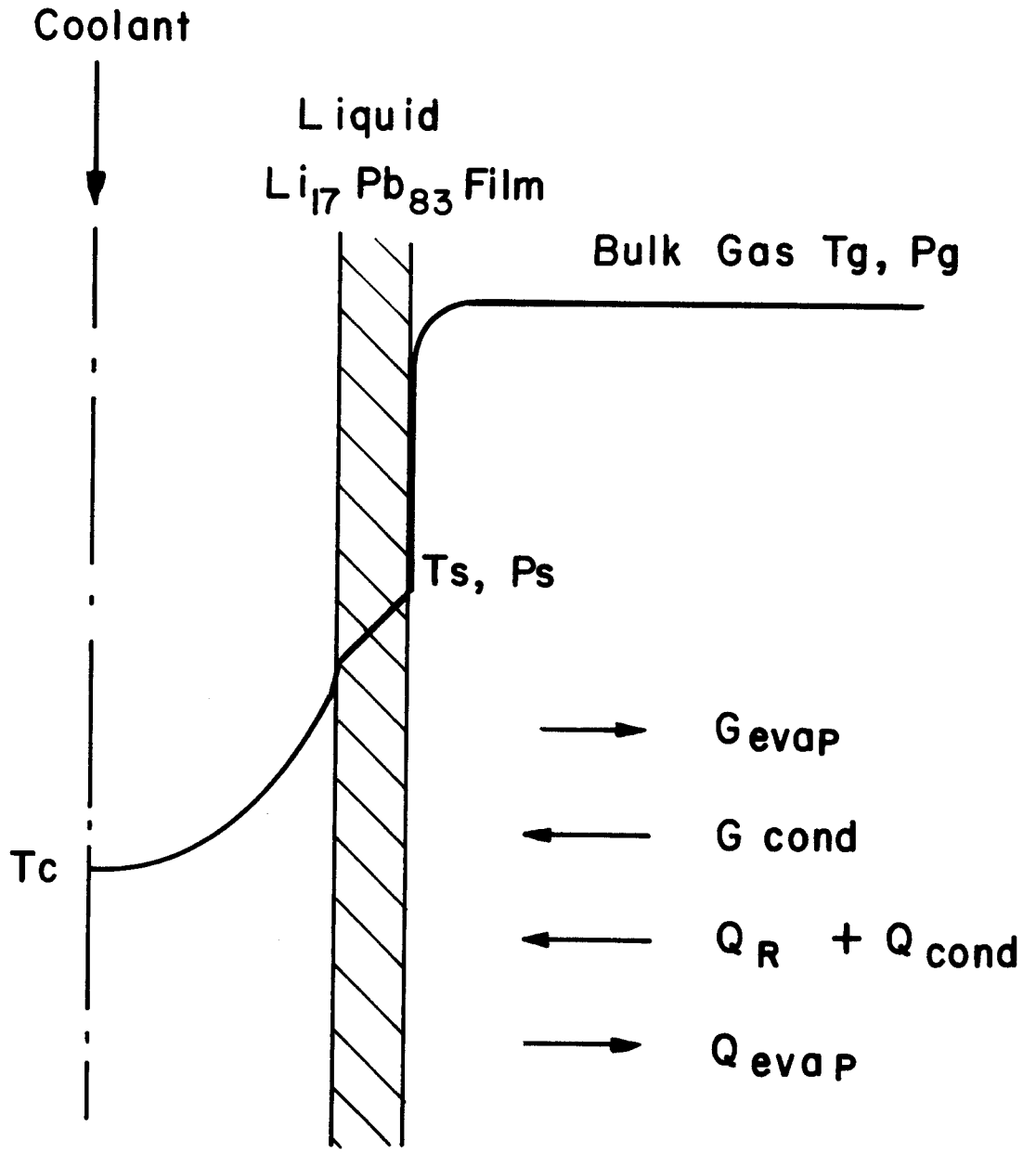

Figure 4 The exchange of mass, energy between the bulk gas and the first surface.

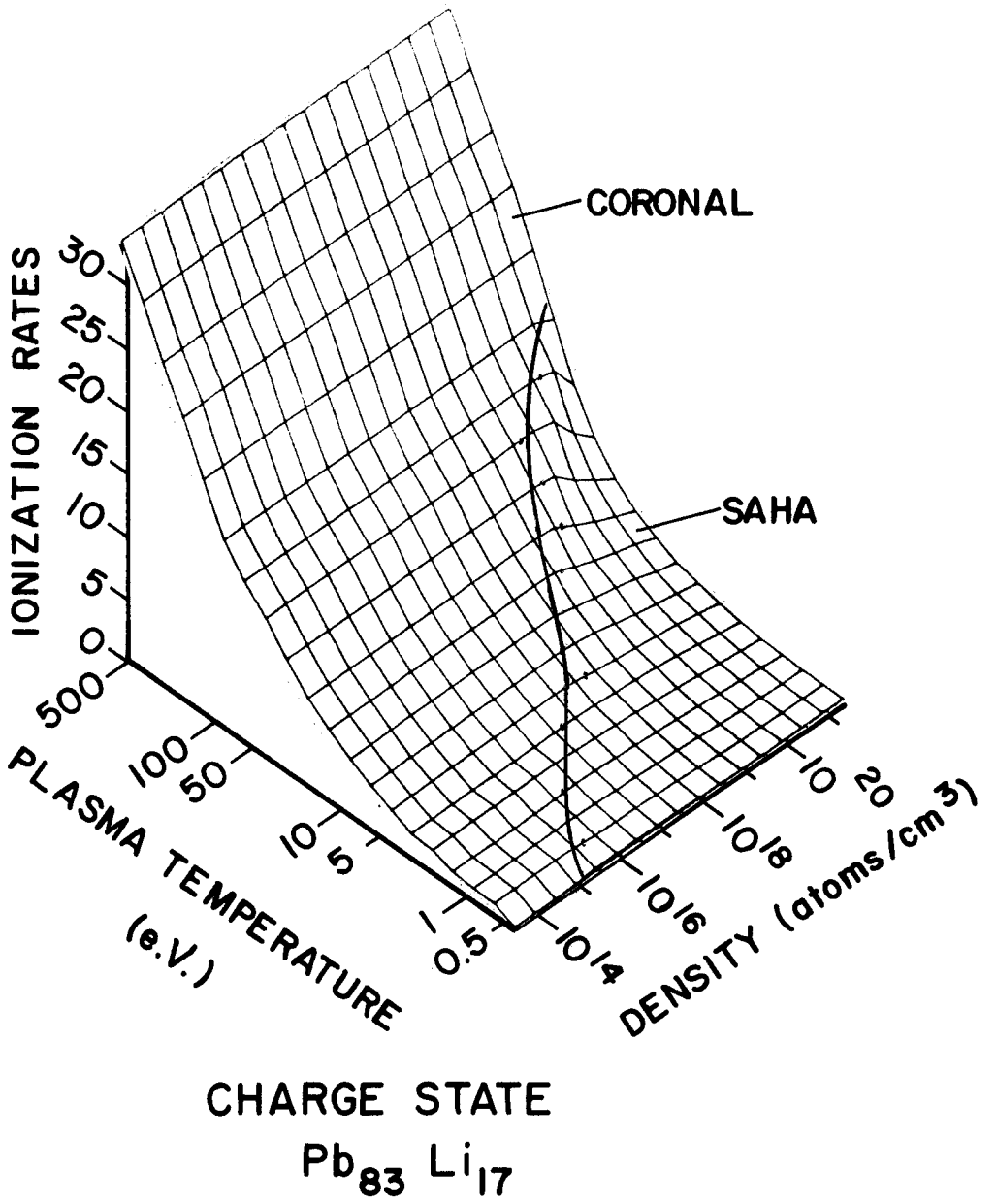

Figure 5 Ionization state for $Li_{17}Pb_{83}$ in Saha and Coronal model.

(i) Condensation:

$$G_{cond} = \left(\frac{M}{2\pi R}\right)^{1/2} \frac{P_g}{T_g^{1/2}}$$

$$Q_{cond} = G_{cond} * \Delta\theta[\Delta H + C_p(T_g - T_s)]$$

G_{cond}: condensation mass flux

P_g: pressure of the gas

T_g: temperature of the gas

M: molecular weight of Pb

Q_{cond}: energy deposited due to condensation

$\Delta\theta$: time step

ΔH: latent heat of vaporization

C_p: specific heat

(ii) Evaporation:

$$\log P_s(\text{torr}) = -\frac{10130}{T_s} + 11.16 - 0.985 \log T_s$$

for $600°K \leq T_s \leq 2030°K$.

$$G_{evap} = \left(\frac{M}{2\pi R}\right)^{1/2} \frac{P_s}{T_s^{1/2}}$$

$$Q_{evap} = G_{evap}\Delta\theta\Delta H$$

P_s: pressure of the surface

T_s: temperature of the surface

G_{evap}: evaporation mass flux

Q_{evap}: energy loss due to evaporation

(iii) Wall Temperature:

$$-k \frac{dT}{dx} = Q_{tot} = Q_R + Q_{cond} - Q_{evap} \qquad \text{at } x = 0$$

$$k \frac{\partial^2 T}{\partial x^2} = \rho C_p \frac{\partial T}{\partial \theta} \qquad 0 < x < x_o$$

$$-k \frac{dT}{dx} = h(T - T_c) \qquad \text{at } x = x_o$$

k: thermal conductivity of $Pb_{83}Li_{17}$

ρ: density

Q_R: energy deposited due to radiation

x: the distance from the surface

x_o: the thickness of the film

h: heat transfer coefficient

T_c: coolant temperature

(iv) Mass Change:

$$\frac{dm_{bulk}}{dt} = (G_{evap} - G_{cond}) * A$$

m_{bulk}: total mass of the bulk gas

A: the surface area of the reactor chamber

(v) Initial Conditions:

m_{bulk}:	13000 g
T_g:	1.3 eV

Wall temperature (°C): $T(x) = 1427 \exp(-6666.67\ x) + T_c$

III. Calculation Results for 13 kg Initial Mass

For 13 kg initial evaporated mass after the x-ray deposition, the calculation results are shown in Figs. 6-9. Figure 6 shows the hydrodynamic motion of the $Pb_{83}Li_{17}$ gas. At about 1 msec, the gas reaches the cavity center. Figure 7 shows the surface heating due to radiation, evaporation and condensation. At the beginning the radiation and evaporation dominate; later, the condensation dominates. The peaks in the figure occur because at this time, the gas reaches the center and we assume that the gas converts its kinetic energy into heat. Figures 8 and 9 show the history of the gas density with the old calculation and the improved calculation in linear and logarithmic plots. From these results, we can summarize the whole gas dynamic process into 9 stages, and show it in Fig. 3.

1. Target explosion.
2. The film is vaporized by the x-rays.
3. The vapor begins moving toward the target and absorbs the energy of the ions. After about 10^{-4} sec, the vapor temperature is raised to about 1.3 eV.
4. The gas continues flowing toward the center and begins radiating energy onto the INPORT tubes.
5. Additional $Pb_{83}Li_{17}$ is evaporated off of the tubes by this radiation heat flux.
6. The radiation heat flux reaching the tube surface is decreasing because of the increased amount of vaporized mass increasing the opacity of the gas.

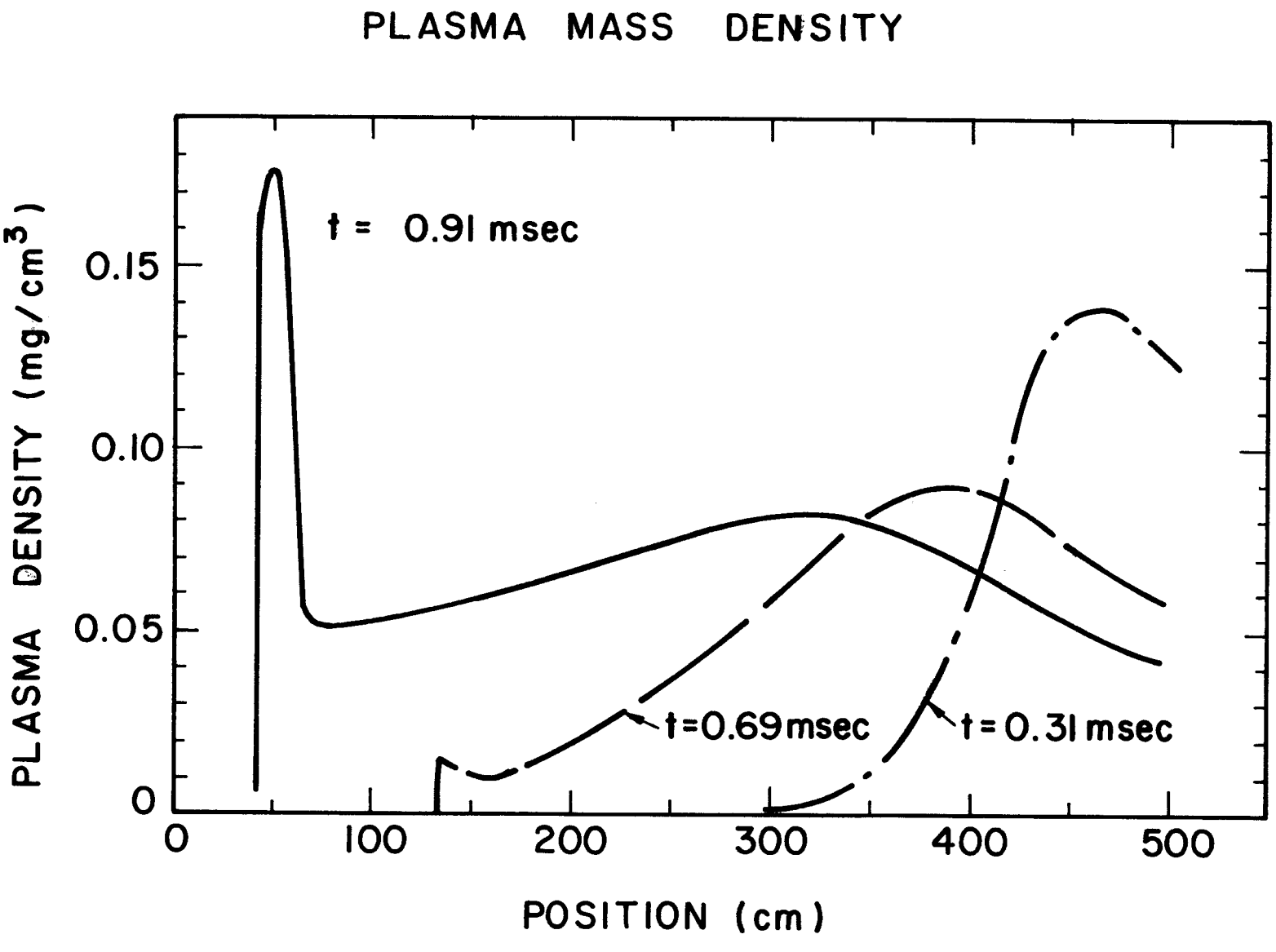

Figure 6 Hydrodynamic motion of $Li_{17}Pb_{83}$ vapor moving from tubes to cavity center.

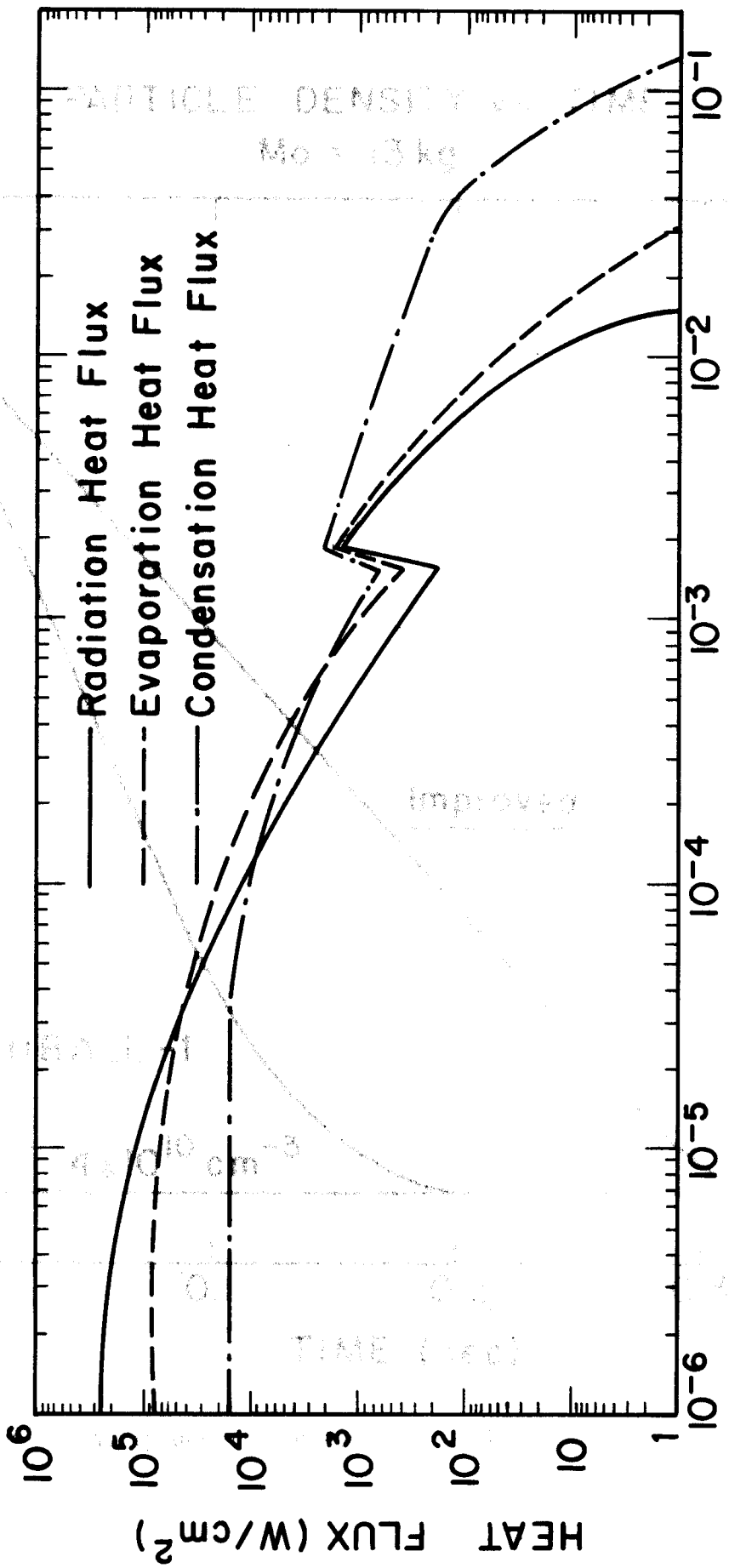

Figure 7 First surface heat flux from radiation, condensation and evaporation.

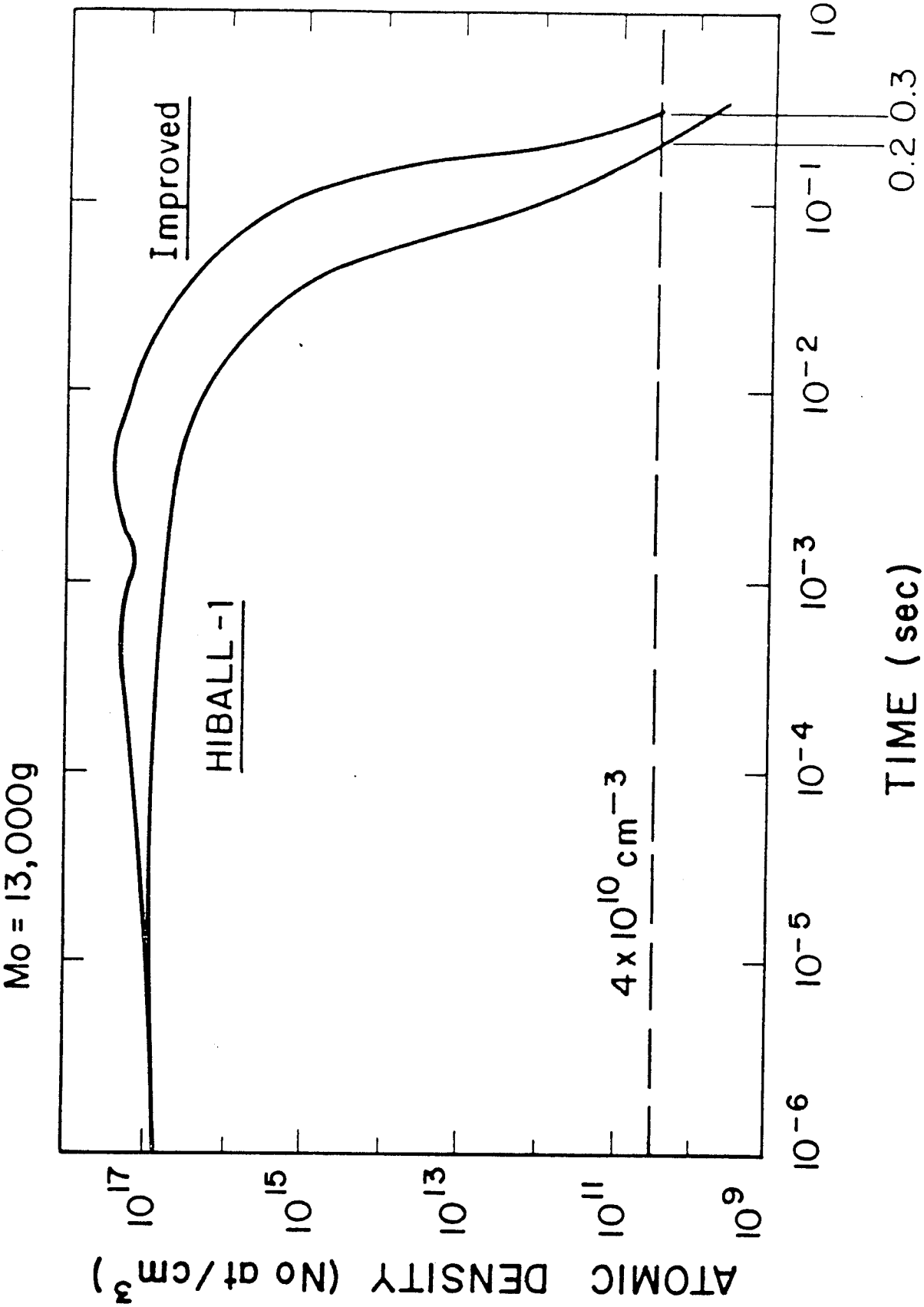

Figure 9 Cavity density versus time -- logarithmic plot.

7. Around 1 msec, the gas reaches the center and converts its kinetic energy into heat. This causes much $Pb_{83}Li_{17}$ evaporation.
8. The cooling gas condenses back onto the tubes.
9. After about 0.3 sec, the gas density will be below $4 \times 10^{10}/cm^3$.

IV. Conclusion and Comments

For HIBALL-I with 5 Hz repetition rate, our calculation shows that at 0.2 sec, the gas density is about $9 \times 10^{12}/cm^3$. However, we note that there are some uncertainties involved in this calculation. From the target burn calculation, we know the total energy (includes x-ray and debris) input to the first surface should be 34.5 J/cm^2. At the end of our calculation, we got only 26.9 J/cm^2. This means we have a cooler gas than we actually predicted. If we have a hotter gas, the radiation heat flux will be higher, and there will be more gas evaporated. Also a hotter gas might have a higher kinetic energy. It will move to the surface more quickly, causing a higher condensation rate. There are a number of assumptions made in this analysis that require further study. For large condensation and evaporation rates we must modify assumptions 9 and 10. Furthermore, we now believe that the presence of non-condensible gases (T, D, and He) will have an effect on the condensation rate so that assumption 11 may not be fully justified.

The results presented here show that the gas recondenses to below 4×10^{10} cm^{-3} in 0.3 seconds and thus the maximum repetition rate is ~ 3 Hz. However, the above discussion indicates that we are only beginning to understand this complex dynamic phenomenon and work is continuing to gain better insight into this problem.

References

1. B. Badger et al., "HIBALL - A Conceptual Heavy Ion Beam Driven Fusion Reactor Study," KfK-3202/1, UWFDM-450 (December 1981).

2. G.L. Kulcinski et al., "The INPORT Concept - An Improved Method to Protect ICF Reactor First Walls," University of Wisconsin Fusion Engineering Program Report UWFDM-426 (August 1981).

3. R.R. Peterson et al., "Gas Dynamics in Liquid Metal ICF Reactor First Wall Surfaces," University of Wisconsin Fusion Engineering Program Report UWFDM-443 (October 1981).

4. G.A. Moses and R.R. Peterson, "FIRE - A Computer Code to Simulate Cavity Gas Response to Inertial Confinement Target Explosions," University of Wisconsin Fusion Engineering Program Report UWFDM-336 (January 1980).

5. D. Mikalas, Stellar Atmoshperes, W.H. Freeman and Co., San Francisco, 1978.

6. D. Mosher, NRL Memorandum Report 2563 (March 1973).

7. Ya B. Zel'dovich and Yu. P. Raizer, Physics of Shock Waves and High Temperature Hydrodynamic Phenomena, Chap. III, Academic Press, New York, 1967.

ACKNOWLEDGMENT

Support for this work has been provided by the Kernforschungszentrum Karlsruhe and the Bundesministerium für Forschung und Technologie, Federal Republic of Germany, under research agreement with Fusion Power Associates, Gaithersburg MD.